Current Zoology, 2018, 64(6), 765–773
doi: 10.1093/cz/zoy005
Advance Access Publication Date: 12 January 2018
Article

Article

Brain of the blind: transcriptomics of the golden-line cavefish brain

Fanwei Meng[a,*], Yahui Zhao[b], Tom Titus[c], Chunguang Zhang[b], and John H. Postlethwait[c,*]

[a]State Key Laboratory of Membrane Biology, Institute of Zoology, Chinese Academy of Sciences, Beijing 100101, China, [b]Key Laboratory of Zoological Systematics and Evolution, Institute of Zoology, Chinese Academy of Sciences, Beijing 100101, China, and [c]Institute of Neuroscience, University of Oregon, Eugene, OR 97403, USA

*Address correspondence to Fanwei Meng. E-mail: mengfw@ioz.ac.cn and John H. Postlethwait. E-mail: jpostle@uoneuro.uoregon.edu.

Received on 7 November 2017; accepted on 9 January 2018

Abstract

The genus *Sinocyclocheilus* (golden-line barbel) includes 25 species of cave-dwelling blind fish (cavefish) and more than 30 surface-dwelling species with normal vision. Cave environments are dark and generally nutrient-poor with few predators. Cavefish of several genera evolved convergent morphological adaptations in visual, pigmentation, brain, olfactory, and digestive systems. We compared brain morphology and gene expression patterns in a cavefish *Sinocyclocheilus anophthalmus* with those of a closely related surface-dwelling species *S. angustiporus*. Results showed that cavefish have a longer olfactory tract and a much smaller optic tectum than surface fish. Transcriptomics by RNA-seq revealed that many genes upregulated in cavefish are related to lysosomes and the degradation and metabolism of proteins, amino acids, and lipids. Genes downregulated in cavefish tended to involve "activation of gene expression in cholesterol biosynthesis" and cholesterol degradation in the brain. Genes encoding Srebfs (sterol regulatory element-binding transcription factors) and Srebf targets, including enzymes in cholesterol synthesis, were downregulated in cavefish brains compared with surface fish brains. The gene encoding Cyp46a1, which eliminates cholesterol from the brain, was also downregulated in cavefish brains, while the total level of cholesterol in the brain remained unchanged. Cavefish brains misexpressed several genes encoding proteins in the hypothalamus–pituitary axis, including Trh, Sst, Crh, Pomc, and Mc4r. These results suggest that the rate of lipid biosynthesis and breakdown may both be depressed in golden-line cavefish brains but that the lysosome recycling rate may be increased in cavefish; properties that might be related to differences in nutrient availability in caves.

Key words: cavefish, cholesterol, cyp46a, optic tectum, *Sinocyclocheilus*, transcriptomics.

Caves present organisms with an extreme environment, but various lineages of fish have independently colonized these perpetually dark realms. Teleost fish from at least 19 families have successfully colonized caves from 40°N to the Tropic of Capricorn (Zhao et al. 2011). Cave-dwelling fish have evolved a suite of troglomorphic traits, including reduction or loss of eyes, pigmentation, and scales, coupled with the enhancement of chemoreceptors in olfactory organs and mechanoreceptors including the lateral-line system (Protas et al. 2008; Windsor et al. 2008; Jeffery 2009; Romero et al. 2009; Gross 2012; Krishnan and Rohner 2017). Among cavefish species, investigations of the Mexican tetra *Astyanax mexicanus* have led to many important advancements concerning the evolution of troglodyte traits, for example, the eyes and optic tectum of *Astyanax* cavefish are greatly reduced (Rohner et al. 2013; Elipot et al. 2014; McGaugh et al. 2014; Simon et al. 2017; Stahl and Gross 2017).

'The cyprinid *Sinocyclocheilus* (golden-line barbel) is the most species-rich cavefish genus with more than 55 known species, about 25 of which live in energy-limited cave environments (Romero et al. 2009; Zhao et al. 2011; Meng et al. 2013 b; Yang et al. 2016). Phylogenetic analyses based on mitochondrial *cytochrome b* and *ND4* gene sequences have shown that the known *Sinocyclocheilus* species cluster into 5 major monophyletic clades (Xiao et al. 2005), several of which have cave-dwelling forms, suggesting that different lineages of *Sinocyclocheilus* have adapted to cave environments independently several times. Comparative transcriptomic and genomic analyses of *Sinocyclocheilus* species have revealed many genetic changes that were associated with adaptive features such as eye degeneration, albinism, rudimentary scales, circadian rhythm, and enhanced taste buds (Meng et al. 2013a; Yang et al. 2016). Thus, *Sinocyclocheilus* provides an ideal model genus to evaluate the mechanisms of adaptation in cave animals.

Like cavefish, some people are born blind and the brains of blind people develop a compensatory reorganization, especially in areas that appear to help improve spatial resolution of sounds (Roder et al. 1999). Similar types of brain reorganization may occur in blind cavefish. Several studies have investigated the eye, brain, and behavior in cavefish (Soares et al. 2004; Menuet et al. 2007; Yoshizawa et al. 2010; Strecker et al. 2012; Yoshizawa et al. 2015). These studies show that cavefish have a larger hypothalamus region, reduced the size of the optic tectum, well-developed olfactory bulbs, and more sensory hair cells in the neuromasts of the lateral line system. An additional feature of many cave habitats is low and sporadic nutrient availability, and several studies have investigated cavefish energy metabolism. For example, Meng et al. (2013a) found that several genes in the mitochondrial genome that are relevant to energy metabolism are downregulated in the cavefish eye. These results raised the hypothesis that these adaptations contribute to the regulation of energy metabolism in golden-line cavefish in their perpetually dark, clear, slow moving, and presumably nutrient-poor streams, where bat guano or periodic flooding are the only sources of outside nutrients. Although the brain expends a substantial fraction of an animal's whole-body energy budget (Ivanisevic and Siuzdak 2015), it is unknown whether energy metabolism in the cavefish brain has adapted to the food-limited cave environment. This situation led us to wonder how the greatly reduced eyes in congenitally blind golden-line cavefish (Meng et al. 2013a, 2013 b), which would be pathogenic in a surface-dwelling fish, would affect brain structure and gene expression patterns over evolutionary time.

In this study, we first showed that the volume of the optic tectum was significantly smaller in the cavefish *Sinocyclocheilus anophthalmus* than in the surface fish *S. angustiporus* and the length of the olfactory tract was significantly greater in cavefish than in surface fish. Next, to quantify differences in gene expression, we compared the transcriptomes of surface and cavefish by RNA-seq analyses. We identified differentially expressed genes, and found that upregulated genes in the cavefish brain were involved in several pathways related to the lysosome and the degradation and metabolism of proteins, amino acids, and lipids. Downregulated genes in cavefish brains included the sterol regulatory element-binding transcription factor genes (*srebf1*, *srebf2*) and their transcriptionally regulated targets involved in cholesterol biosynthesis, and in addition *cyp46a1*, which encodes the enzyme responsible for cholesterol elimination from the brain. Direct measurements of cholesterol levels showed no differences between cavefish and surface fish brains, suggesting that decreased biosynthesis and decreased degradation of cholesterol balanced each other. We speculate that transcriptome evolution in the cavefish brain may have led to energy savings in cholesterol metabolism, which might help this species to adapt to a presumably resource-poor cave environment.

Materials and Methods

Animals

Golden-line cavefish *S. anophthalmus* were collected in Jiuxiang cave, Yiliang County (N 25.05478°, E 103.37975°, Yunnan, China) and maintained in the laboratory in a dark environment. The surface species, *S. angustiporus* were collected from Huangnihe River in Agang Town (N 25.00905°, E 103.59256°, Yunnan, China). Both collection sites were in the Nanpanjiang River drainage, the largest tributary of Xijiang River in the Pearl River basin. Although the two sites are only about 30 km apart in a straight line, they are separated by about 100 river-kilometers (Supplementary Figure S1). The obligatory cave species and the surface species are closely related phylogenetically (Xiao et al. 2005; Zhao and Zhang 2009) and the sequences of their orthologs are highly similar, 98.12 ± 0.9% identical at the nucleotide level (Meng et al. 2013a), suggesting that differences between them in terms of gene expression levels are more likely to be due to evolved differences adapting to habitat rather than to random neutral differences that occur over time. While the two congeners *S. grahami* and *S. tingi* are more closely related to *S. anophthalmus* than is *S. angustiporus*, unfortunately, these more closely related species are not available in sufficient numbers to perform the required experiments. Surface animals were maintained on a 12: 12 Light: Dark cycle. Cave and surface fish were fed twice per day with the same carp food (Sanyou Chuangmei company, Beijing) in mini pellets, which delivered a nutritionally complete formula. Uneaten food was removed 15 min after feeding. All experimental procedures involving animals were conducted and approved by the Animal Care and Use Committee of Institute of Zoology, Chinese Academy of Sciences.

Brain volume analysis

To investigate the effects of constant darkness on brain morphology, we measured various regions of cavefish and surface fish brains. Surface fish and cavefish were euthanized with 0.05% tricaine methanesulfonate and decapitated (3 individuals per species). The dorsal surface of the head was dissected away to expose the brain directly to prefix in 4% paraformaldehyde (PFA) for 6 h, and then brains were dissected from the head, fixed again in 4% PFA overnight at 4 °C, and finally embedded in paraffin. Transverse sections (10 μm thick) of whole brains of both species were mounted and stained with hematoxylin and eosin. The area of various regions of the brain was measured on every 8th section (80 μm) using ImageJ (version 10.2). The volume was estimated by calculating the area of each section and the distance between the sections (Rosen and Harry 1990). To measure the volume of different brain regions, we calculated the volume of 6 brain areas (olfactory bulb, telencephalon, diencephalon, optic tectum, cerebellum, and medulla oblongata). The telencephalon has two subdivisions, the area dorsalis and the area ventralis telencephali; cerebellum measurements encompassed the crista cerebellaris, corpus cerebelli, and valvula cerebelli. The diencephalon and medulla oblongata were distinguished by the nuclei of the preglomerular complex. The end of the medulla oblongata was the medial funicular nucleus. The volume of different brain regions was normalized to fish standard length (from the tip of the snout to the end of the caudal peduncle). Statistical analysis was performed using a two-tailed Student's *t*-test in Microsoft Excel. All data met the assumption of normality.

Differential gene expression analysis

To obtain insights into the molecular genetic mechanisms involved in the evolution of the cavefish brain, we profiled gene transcription in dissected brains. We generated total RNA from the brain of two adult

individuals of each species (surface and cave dwelling species). Poly $(A)^+$ RNA was isolated from total RNA samples using MicroPoly(A) PuristTM (Ambion) according to the manufacturer's protocol. Brain cDNA libraries were obtained from two individuals for each species following established protocols (Meng et al. 2013a). Samples (200- to 400-bp inserts) were sequenced using 80-nt paired-end reads from an Illumina sequencer GA-II (Illumina Inc., San Diego, CA, USA).

Barcodes were identified and nucleotides with low-quality base calls were removed, and then reads were mapped to the previously assembled golden-line transcriptome (Meng et al. 2013a) using Bowtie (Langmead 2010). In Bowtie, "the maximum mismatches per read" was set to 3 while other parameters were left as default. Accession numbers are GAHO01000000 for *S. angustiporus* and GAHL01000000 for *S. anophthalmus* at DDBJ/EMBL/GenBank. Mapped reads of both surface and cave species were converted to RPKM (reads per kilobase of exon per million mapped sequence reads) values and normalized (Mortazavi et al. 2008). To enhance statistical robustness, genes with fewer than 5 RPKM in either species were excluded from the pathway enrichment and gene ontology (GO) analyses, but these genes are recorded in a subsheet of Supplementary Table S1. *P*-values were obtained for each gene by computing a conditional probability of observing N1 reads for a gene given that we obtained N2 reads from the controls and experimentals (Audic and Claverie 1997). Genes were identified as differentially expressed when fold change (FC) was >2 and $P<0.05$. We used WebGestalt (Wang et al. 2013) to identify functional categories among the differentially expressed genes.

Real-time polymerase chain reaction

cDNA samples were created from mRNAs isolated from the brains of surface and cave-dwelling individuals. Real-time polymerase chain reaction (PCR) was conducted using SYBR Green (TaKaRa) chemistry. Real-time PCR primers were designed based on the golden-line transcriptome sequence assembled previously (Meng et al. 2013a). Primer sequences were as follows (forward and reverse): *β-actin*: 5′-GAA GATCAAGATCATTGCTCCC-3′ and 5′-ATGTCATCTTGTTCGAG AGGT-3′; *cyp46a1.3*: 5′-GGAAACGCTGCGTCTGTA-3′ and 5′-GG TTCGTGGACCAAGTGC-3′; *cyp51*: 5′-CATCCTGCAAACGCTGAT AG-3′ and 5′-AGTGCAGAGGAGGCAGATGT-3′; *dhcr24*: 5′-ATGG GAACAGGCATTGAGTC-3′ and 5′-TAGCGAAGCTTCACCCAT TT-3′; *ebp*: 5′-AACGCGGGAAATAATCACAT-3′ and 5′-TGAAC GGTCATTAGCCACAT-3′; *faxdc2*: 5′-GTTGTTTAACGCCCTCC TGA-3′ and 5′-CGCCTCTTCATCACCATGTA-3′; *fdft1*: 5′-TGGG TCTGTTCCTCCAGAAG-3′ and 5′-TCTGGGACGTGATGGAGAG-3′; *fdps*: 5′-CTCCTGGAGGCAAGAGAAAC-3′ and 5′-ATGTCAT CAGCCACCAAGAA-3′; *hmgcra*: 5′-CCCAAGAGAATTGAGCCA GA-3′ and 5′-CAGCACTGATCAGGAGACCA-3′; *hmgcs1*: 5′-GGGA TGATCAAGGAGATCCA-3′ and 5′-CAACACTGGACTGGGAT TAGC-3′; *nsdhl*: 5′-GGAACCGACATCAAGAATGG-3′ and 5′-GC GGGCTGTATCTATCAGGA-3′; *pmvk*: 5′-ATAGATGTGTCTGCGT TCGG-3′ and 5′-TTCTCCAGAACGTCATCAGC-3′; *srebf1*: 5′-GATT GGATGTTGCCCACTCT-3′ and 5′-GACGACCAAGAGCTTTGAG G-3′; *srebf2*: 5′-CTCTCCTGGAACCTGATTCG-3′ and 5′-AGACA CACACACACCCCAGA-3′; *tm7sf2*: 5′-TCGGGTATCTGTTTGAG CTG-3′ and 5′-CTCGACCCATGAAGAAGTCA-3′. We used *βsed in* as a reference gene. All PCR reactions were run in a 96-well block with 20 μL reactions in each well. All assays included reference samples and negative controls in which cDNAs were replaced by water. Target genes were normalized to the reference gene and expression levels were quantified using the relative Ct method. Each reaction (samples and primers) involved at least 3 replicates.

Identification of enriched pathways

Enriched pathways were identified from differentially expressed genes in the brains of cavefish and surface fish using KOBAS 3.0 (updated 26 January 2015) (Xie et al. 2011), a program that assigns putative pathways and disease relationships to a gene set and provides statistically significant enriched pathways from 5 pathway databases. Sequences of differentially expressed genes were compared to the *Homo sapiens* database using the "annotate" feature in KOBAS 3.0 to allow inferences from the data on human pathways. We then used "identify" to find significantly enriched pathways; "inputs" were the output of "annotate" for upregulated and downregulated gene sets, and the "background" was the entire set of 11,471 unique genes expressed in the golden-line brain identified by RNA-seq. Data were analyzed using a hypergeometric test and Benjamini–Hochberg FDR (false discovery rate) correction, and only pathways or diseases with a corrected $P<0.05$ were considered to be enriched.

Cholesterol content

Brain, liver, and muscle tissues of cavefish and surface fish were homogenized in 50 mM NaCl. The lipid fraction was then extracted through multiple washes with a 2:1 chloroform: methanol solution. Samples were dried down with 10% triton-X 100/acetone (Suzuki et al. 2013). Cholesterol content was assayed by enzymatic assay according to the manufacturer's protocol (Wako Chemicals, cat: 439-17501).

Results

The optic tectum is smaller in cavefish than in surface fish

The cave-dwelling species *S. anophthalmus* has small internal eyes in contrast with those of its closely related surface-dwelling species *S. angustiporus* (Figure 1A,B, Supplementary Figure S2A). Laser light (wavelengths are 650 nm for red and 532 nm for green) was shined into the eyes of cavefish and surface fish. Surface fish responded by moving to avoid the light. In contrast, cavefish treated in the same way made no response (cavefish $n=12$, surface fish $n=9$). We conclude that the eyes of cavefish do not detect light or that cavefish fail to react to light.

Measurements showed that cavefish brains were slimmer than those of surface fish (Figures 1C,D and 2A). The results of brain morphological analysis showed that the volume of the optic tectum in golden-line cavefish was significantly smaller than in surface fish, about a third as large (Figures 1E,F and 2B), a result also found in *Astyanax* cavefish. In addition to a difference in the volume of the optic tectum, the olfactory tract was over twice as long in cavefish than in surface fish (2.46 ± 0.12-fold longer in cavefish than surface fish) (Figures 1C,D and 2C). This change in brain morphology reflects differences in the morphology of the whole head in cavefish and surface fish (Figure 1A,B, Supplementary Figure S2B), because the head of cavefish ($30.9\%\pm0.9\%$ of standard length) was longer than the head of surface fish ($27.2\%\pm1.0\%$) (Head length: the distance between the snout tip and posterior edge of operculum).

Brain volume analysis has shown that the volume of the optic tectum was significantly smaller (Figure 2B: $33.4\pm1.4\%$, $P<0.001$) in cavefish than in surface fish. The volume of the other 5 brain regions was not significantly different while comparing cavefish to surface fish (Figure 2B, $P>0.05$). These results are consistent with the hypothesis that reduced inputs of visual signals led to a reduction in the volume of the optic tectum in the cavefish.

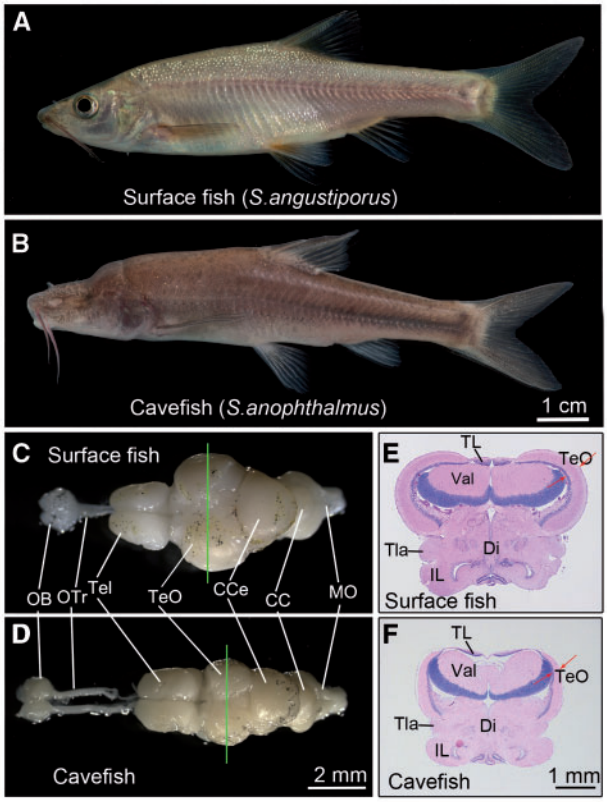

Figure 1. Cavefish phenotypes. Surface fish *S. angustiporus* (A) and cavefish *S. anophthalmus* (B). Dissected brains of surface (C) and cavefish (D). Green lines indicate the locations of sections in E and F. Hematoxylin and eosin stained sections of adult surface fish brain (E) and cavefish brain (F). CC: crista cerebellaris; CCe: corpus cerebelli; Di: diencephalon; IL: inferior lobe; MO: medulla oblongata; OB: olfactory bulb; OT: optic tectum; OTr: olfactory tract; Tel: telencephalon; TL: torus longitudinalis; Tla: torus lateralis; Val: valvula cerebelli. Scale bar in (A and B): 1 cm; (C and D): 2 mm; (E and F) 1 mm.

Differential gene expression comparing brains of cavefish and surface fish

The Illumina sequencing reads were deposited in the Short Read Archive as accession numbers SRR788094 for *S. angustiporus*; SRR788095 for *S. anophthalmus*. For the cavefish brain, a total of 12,895,766 reads, corresponding to 43.63% of all high-quality cavefish reads, mapped to 55,362 golden-line transcriptome contigs (98.73%) and matched to 13,957 zebrafish UniGenes. For the surface fish brain, 7,642,283 reads (49.66%) mapped to the golden-line transcriptome, which aligned to 53,115 golden-line reference transcriptome contigs (94.72%) and matched to 13,768 zebrafish UniGenes.

We obtained 11,471 unique genes with expression values ≥ 5 RPKM in at least one of the golden-line brain transcriptomes. Among these unique genes, 2,147 were identified as differentially expressed (≥2-FC in transcript level between cavefish and surface fish with a $P < 0.05$). Of the differentially expressed genes, 1,080 were downregulated and 1,067 were upregulated in the cavefish brain. Supplementary Table S1 lists differentially expressed genes.

Of the 1,067 upregulated genes, 949 mapped to unique human Entrez Gene IDs. Of the 1,080 downregulated genes, 758 mapped to unique human Entrez Gene IDs. Enrichment analyses were conducted and GO Slim classifications were assigned based on the mapped unique Entrez Gene IDs (Figure 3). In the biological process category, cavefish gene expression was downregulated relative to surface fish in the subcategories of biological regulation, multicellular organismal processes, developmental processes, cell communication, and growth (Figure 3); in the cellular component category, cavefish were substantially downregulated in the nucleus, extracellular matrix, and chromosome subcategories (Figure 3); and in the molecular function category, cavefish were downregulated in the nucleic acid binding, molecular transducer activity, and chromatin binding subcategories (Figure 3). These differences likely reflect genes that are related to the function and development of the cavefish brain.

Identification of enriched pathways among differentially expressed genes

Results showed that 17 pathways had significant *P*-values (<0.01) in the downregulated gene group and 20 pathways had significant *P*-values (<0.01) in the upregulated group. Pathways relevant to cholesterol biosynthesis were significantly enriched in the downregulated group, including "activation of gene expression by Srebf" (sterol regulatory element-binding protein, Reactome pathway database) and "cholesterol biosynthesis" (Reactome) (Supplementary Table S2). In the upregulated group, 8 of 20 enriched pathways were involved in degradation and metabolism of proteins, amino acids, and lipids. These pathways included "sumoylation" (BioCarta), "lysosome" (KEGG), "phenylalanine and tyrosine catabolism" (Reactome), "eicosanoid metabolism" (BioCarta), and "other glycan degradation" (KEGG) (Supplementary Table S2). These findings suggested that, compared with the surface fish brain, the cavefish brain reduces the synthesis and metabolism of organic compounds and/or enhances the degradation and recycling of materials.

Enhanced material recycling by the lysosome in the cavefish brain

Several genes upregulated in cavefish brains encode members of the adaptor-related protein complex, a part of the clathrin coat assembly [*ap1s1*{3.93 FC up}, *ap1s2* {2.22 up}, *ap1s3b* {3.26 up}, *ap3m1* {3.26 up}, and *ap4s1* {2.52 up}] (Supplementary Table S1). RNA-seq results also showed that lysosome-related genes were significantly upregulated in cavefish brains compared with the brains of surface fish, including genes encoding several lysosomal enzymes, such as *aga* (2.01 up), *asah1a* (3.92 up), *ctsk* (2.89 up), *galcb* (3.54 up), *gla* (2.56 up), *glb1l* (2.16 up), *ppt1* (2.81 up) and, *sgsh* (2.36 up) (Supplementary Table S1). These results suggested that the cavefish brain may be more active in the conduction of materials and destruction of cell components than the surface fish brain.

Reduced expression of genes regulated by srebfs

Genes that were downregulated in the cavefish brain were significantly enriched in the "activation of gene expression by Srebf" pathway (13/41, $P = 0.000091$). In the cavefish brain, 13 genes in the "activation of gene expression by Srebf" category were downregulated, and 7 of these genes encode cholesterol-synthesizing enzymes, *cyp51* (3.51 FC down), *dhcr7* (2.16 down), *fdft1* (4.26 down), *hmgcs1* (7.89 down), *idi1* (2.03 down), *lss* (2.18 down), and *sqle* (5.41 down). Srebp also regulates the nuclear gene encoding mitochondrial glycerol-3-phosphate acyltransferase (*gpam*), which was downregulated (2.04 down). Additional factors that co-activate Srebf target genes were also downregulated, including CREB binding protein a (*crebbpa*, 2.23 down), *crebbpb* (−2.07 down), nuclear receptor coactivator 1 (*ncoa1*, 2.51 down), and retinoid X receptor-α-a (*rxraa*, 2.00 down).

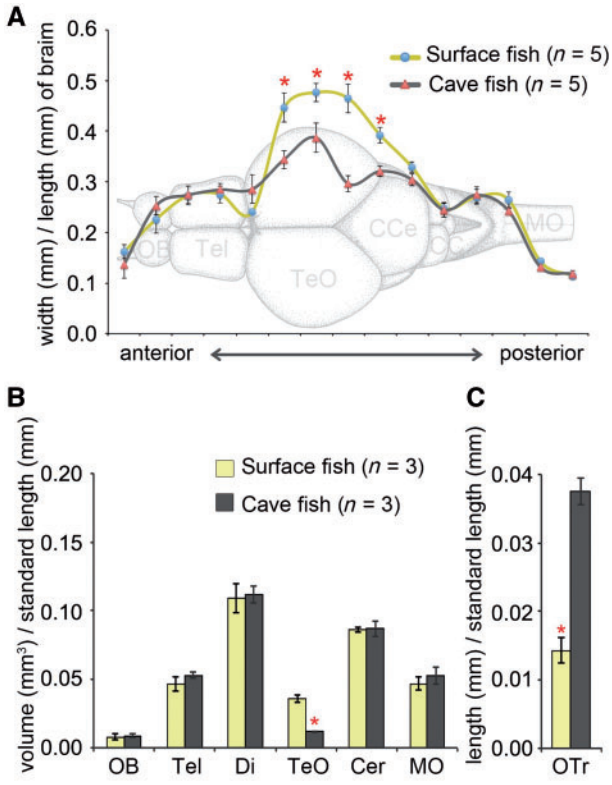

Figure 2. Morphometrics of cavefish brains. (A) Cavefish have a slender brain compared to surface species. (B) Comparison of the volume of different brain regions normalized to fish standard length (excludes the length of the caudal fin of fish). (C) Comparison of the length of olfactory tract to fish standard length. Values expressed as mean ± SD, $*P < 0.01$. CC: crista cerebellaris; CCe: corpus cerebelli; Di: diencephalon; MO: medulla oblongata; OB: olfactory bulb; OTr: olfactory tract; Tel: telencephalon; TeO: optic tectum.

Additionally, in cavefish brains, both *srebf1* and *srebf2* themselves were downregulated (2.90 down and 1.68 down, respectively) with respect to surface fish brains (Supplementary Table S1). Real-time quantitative PCR confirmed the direction and approximate magnitude of gene expression change for all of the 14 genes tested (Figure 4).

Downregulation of genes involved in cholesterol biosynthesis and catabolism in the cavefish brain

RNA-seq analyses revealed that many genes involved in cholesterol biosynthesis were downregulated in the cavefish brain relative to the surface fish brain. Figure 5 displays our RNA-seq results superimposed onto the biosynthetic pathway of cholesterol synthesis. The gene encoding Hmgcr, which catalyzes the rate-limiting step of cholesterol biosynthesis, was downregulated 2.3-fold along with 9 additional enzymes in cholesterol biosynthesis that were significantly reduced in cavefish brain (Figure 5). The gene encoding Pmvk was the only cholesterol synthesis gene that was upregulated (2.51 up, $P < 0.001$) in cavefish brains relative to surface fish brains (Figure 5 and Supplementary Table S1). Many cholesterol biosynthesis genes that were downregulated in the cavefish brain are downstream targets of Srebfs, including *hmgcs1* (7.89 down), *hmgcra* (2.31 down), *sqle* (5.41 down), *fdft1* (4.26 down), *cyp51* (3.51 down), *lss* (2.18 down), *dhcr7* (2.16 down), and *idi1* (2.03 down), suggesting that the downregulation of cholesterol biosynthesis genes is likely to be facilitated by the reduced expression of *srebfs* we found in cavefish brains. The enzyme Cyp46a1 eliminates cholesterol in the brain and our RNA-seq data showed that *cyp46a1* was significantly downregulated (2.91 down) in the cavefish brain relative to the surface fish brain (Figure 4 and Supplementary Table S1).

To test whether the downregulation of genes for both the synthesis and breakdown of cholesterol affect cholesterol homeostasis in cavefish, we extracted lipids from brain, liver, and muscle of both species and assayed their cholesterol content. Results revealed no significant difference between cholesterol levels in the brains, livers, or muscles of cavefish versus surface fish (Figure 6A,B). This result would be expected if the rate of synthesis and the rate of breakdown of cholesterol were both lower in cavefish than in surface fish, as suggested by the RNA-seq data.

Differential expression of genes in the mitochondrial genome and hypothalamic hormones

In the cavefish brain, none of the 13 genes in the mitochondrial genome were downregulated, but 4 genes in the mitochondrial genome were upregulated (*mt-atp6*, 2.08 up; *mt-atp8*, 4.71 up; *mt-co3*, 2.23 up; *mt-nd3*, 2.13 up) (Supplementary Figure S3 and Supplementary Table S1).

Orthologs of 3 of 7 genes encoding secreted hypothalamic hormones were annotated in our RNA-seq dataset, and all 3 were strongly upregulated in golden-line cavefish compared with golden-line surface fish (Supplementary Table S1). Thyrotropin-releasing hormone (*trh*, 2.38 up) and its receptor in the pituitary (*trhrb*, 3.13 up) were significantly upregulated, as was somatostatin (*sst1*, 2.42 up and *sst3*, 4.05 up). Corticotropin-releasing hormone (*crhb*, 4.06 up) was also significantly upregulated, but its downstream target in the pituitary, *proopiomelanocortin* [*pomca* {alias *acth*}], was substantially downregulated (7.16 down). The gene encoding the melanocortin-4-receptor (*mc4r*) was also downregulated (2.68 down) in golden-line cavefish brains relative to surface fish brains.

Discussion

To investigate the effects of a cave habitat on the brain of a cave-adapted species, we first compared brain morphology between golden-line cavefish and golden-line surface fish. Results showed that the cavefish brain is narrower than the surface fish brain. Furthermore, the volume of the optic tectum in the cavefish brain was about a third of the size of the optic tectum in surface fish. Other brain regions, however, were roughly of the same size in the 2 species. Our finding is consistent with previous studies that showed that adult cave-dwelling *Astyanax* is longer and slimmer than that of the surface population and the size of the optic tectum is smaller in *Astyanax* cavefish due to reduced numbers of retino-tectal fibers compared with surface controls (Riedel 1997; Soares et al. 2004). Reduced retino-tectal fiber input and/or enhanced programmed cell death or reduced proliferation of optic tectum cells might also generate the smaller optic tectum of golden-line barbel cavefish. The convergent small-tectum phenotype is consistent with the idea that common changes in brain morphology evolve independently multiple times in cave-dwelling fish, but a gap in our knowledge is whether these common morphologies reflect shared developmental genetic mechanisms. Further research is needed to document the morphology and molecular genetics of brain development during early life stages of obligatory cave-dwelling *Sinocyclocheilus*.

Our RNA-seq results showed that a cave-dwelling fish species differs from surface fish in the expression levels of genes involved in brain lipid metabolism, secretion of hypothalamic peptide hormones, and mitochondrial activity. We found that genes encoding 3

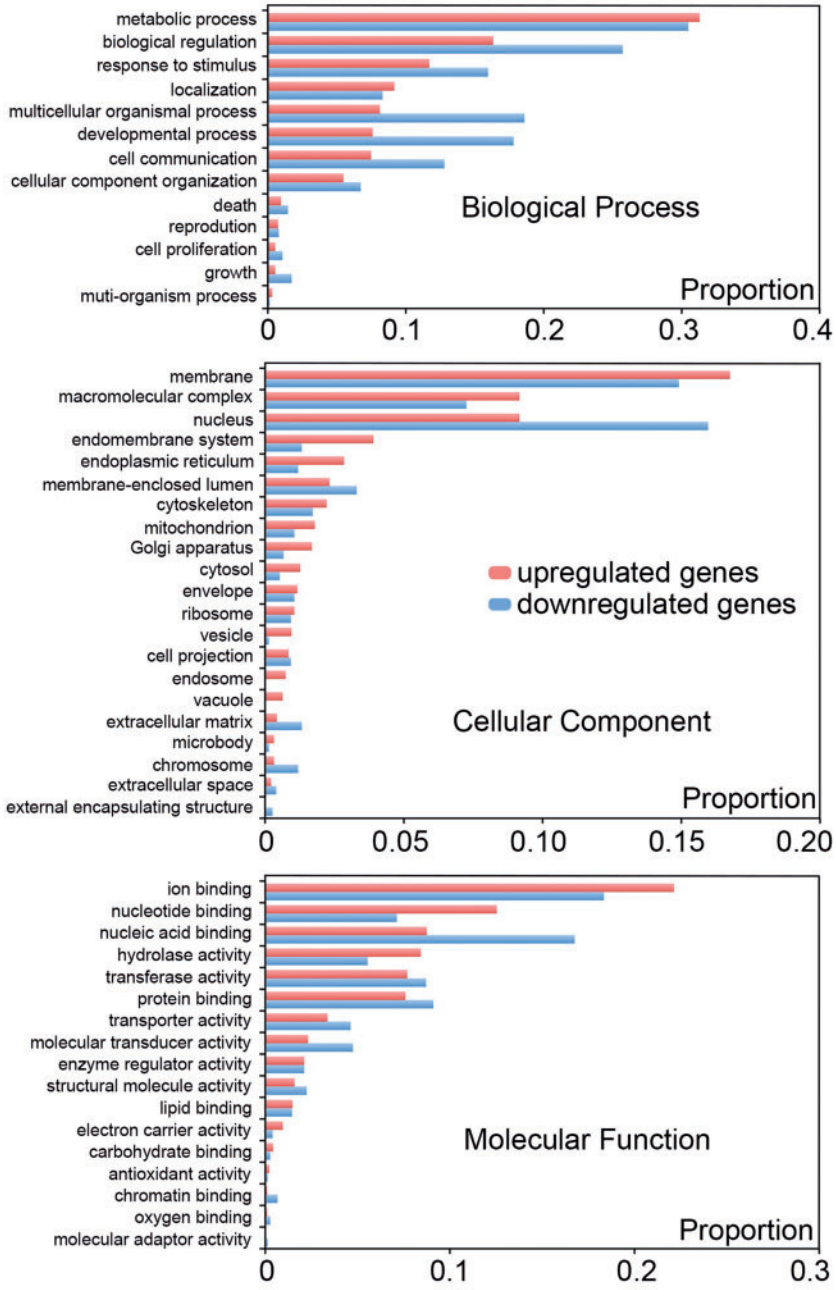

Figure 3. Gene ontology (GO) ID representations for downregulated genes (blue) and upregulated group (red). Three comparisons are shown: biological process ontology, cellular component ontology, and molecular function ontology. Proportion represents the ratio of a gene set in differentially expressed genes compared with a reference gene set in the category.

peptide hormones (Trh, Sst, Crh) secreted by the hypothalamus were upregulated over 3-fold in cavefish compared with surface fish. Trh stimulates the release of thyrotropin (thyroid-stimulating hormone) from the pituitary, which causes the thyroid to produce thyroid hormones, which accelerate metabolism in most cells of the body. Somatostatin (Sst) has an effect opposite to that of Trh: Sst decreases or inhibits the release of thyrotropin from the pituitary (Harris et al. 1978; De Groef et al. 2003; Bodo et al. 2010). The third hypothalamic peptide hormone in our dataset, Crh, is usually secreted in response to stress and it depresses appetite, so its upregulation in the cavefish brain is surprising given the usual expectation that cavefish often have increased appetites (Hüppop 2005). Indeed, mutations have been found in *Astyanax* cavefish in the gene encoding Mc4r (Aspiras et al. 2015), which integrates leptin and insulin levels in the hypothalamus to regulate feeding and metabolism (Tao 2010) and contributes likely to the insatiable appetite of some *Astyanax* cavefish populations (Aspiras et al. 2015); correspondingly, our data showed that *mc4r* expression was downregulated in golden-line cavefish relative to surface fish brains. The upregulation of the pituitary protein Trh-receptor that our data identified might be expected from the upregulation of *thr*, but the upregulation of the hypothalamic gene encoding Crh followed by the downregulation of the gene encoding its downstream hormone Pomc, shows that the regulation of the hypothalamus–pituitary axis in cavefish is likely to be complex and

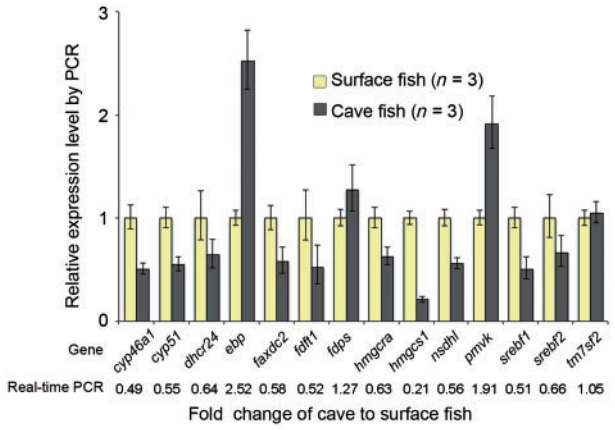

Figure 4. Validation of RNA-seq results by real-time PCR using RNA isolated from brains of each species. Expression levels of target genes were quantified and normalized to *beta-actin1*. Relative expression values are mean ± SD of at least 3 independent experiments.

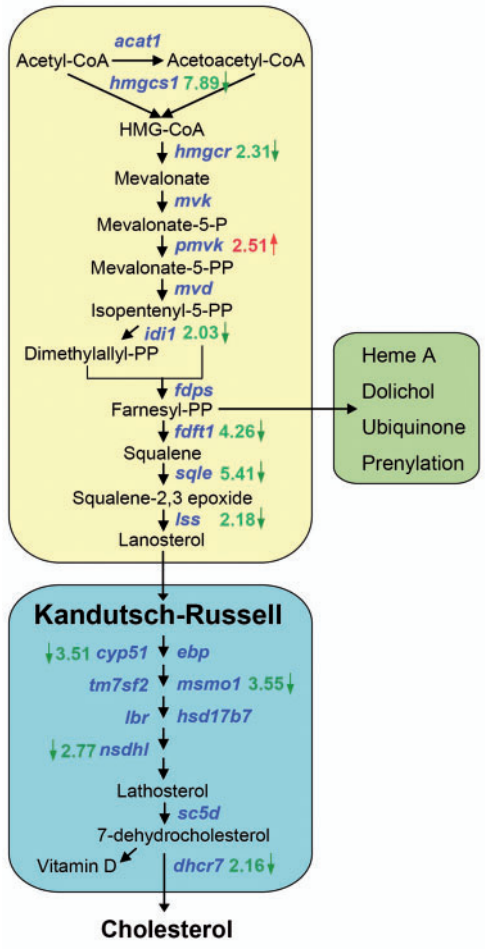

Figure 5. Cholesterol biosynthetic pathway and relative expression changes for genes encoding related enzymes. Hmgcr catalyzes the rate-limiting step of cholesterol biosynthesis. Because the two post-lanosterol pathways (Bloch vs. Kandutsch–Russell) share enzymatic stages, the figure shows only the Kandutsch–Russel pathway, which is the one the brain uses most (Mitsche et al. 2015). Numbers following genes indicate the values of FCs of gene expression. Red numbers and arrows represent upregulation of cavefish relative to surface fish. Green numbers and arrows represent downregulation of cavefish relative to surface fish ($P < 0.01$). P: phosphate, PP: pyrophosphate.

might not be fully described by examining gene expression at the level of mRNA rather than protein.

Experiments reported here revealed low expression of *srebf* genes and downregulation of downstream target genes of *srebfs* in the golden-line cavefish brain. These reduced gene expression levels may lead to decreased cholesterol biosynthesis in the cavefish brain. Cholesterol is a key component of cell membranes that is important for the maintenance and function of neurons and is most concentrated in the brain (Pfrieger 2003; Dietschy and Turley 2004). Correspondingly, Srebf transcription factors can activate the expression of at least 30 genes involved in cholesterol and lipid synthesis (Weber et al. 2004; Porter and Herman 2011; Faust and Kovacs 2014; Martin et al. 2014; Mitsche et al. 2015). The cholesterol content of the brain, however, was similar between cavefish and surface fish brains (Figure 6B), and the likely reason for similar cholesterol contents despite different levels of expression of cholesterol biosynthesis genes is the decreased expression our data show for the gene encoding Cyp46a1, which is the enzyme responsible for eliminating most of the cholesterol removed from the central nervous system (Lund et al. 2003; Russell et al. 2009). Cavefish inhabiting karstic caves, which lack production by autotrophs and experience only sporadic food availability, often exhibit behaviors that maximize energy intake and minimize energy expenditure (Hüppop 2005; Salin et al. 2010). Reduced expression of cholesterol biosynthetic genes might help to reduce energy expenditure in golden-line barbel cavefish.

An additional measure of energy metabolism is the expression level of mitochondrial genes. Our golden-line RNA-seq experiments showed that 4 genes in the mitochondrial genome were upregulated in the cavefish brain. This result for the golden-line cavefish brain contrasts with previous results for the golden-line cavefish eye, in which 7 mitochondrial genes were downregulated with respect to the eye of surface fish (Meng et al. 2013a). Decreased mitochondrial activity in the cavefish eye is likely related to reduced eye size, its internal location, and diminished function; in contrast, increased activity of mitochondrial genes in the brain may reflect increased effort directed toward detecting the environment by nonvisual sense organs, such as lateral line organs and other detectors in the skin, which are increased in some cavefish (Yoshizawa et al. 2010). While changes in the activity of mitochondrial genes may represent adaptations for survival in cave conditions, this hypothesis requires testing by direct measurements of energy expenditures.

Compared with surface aquatic habitats, cave habitats are often nutrient-poor and have seasonal periods of nutrient input (Aspiras et al. 2015). Adaptations to fluctuating environments in *Astyanax* cavefish appear to include a highly efficient metabolism (Moran et al. 2014), and in golden-line cavefish, some of this energy efficiency might involve lower rates of both the synthesis and the breakdown of cholesterol, and/or enhanced degradation and recycling of cellular debris by lysosomes, which contain several enzymes whose genes were upregulated in our data. Studies examining energy expenditures over the entire animal have not yet been conducted in golden-line cavefish and surface fish, so we do not yet know whether the total energy budget of golden-line cavefish is reduced compared to surface congeners, however, the changes we observed in the cavefish brain transcriptome could contribute to more efficient use of limited and sporadic resources in cave environments.

Ethics Statement

All experimental procedures involving animals were conducted and approved by the Animal Care and Use Committee of Institute of Zoology, Chinese Academy of Sciences.

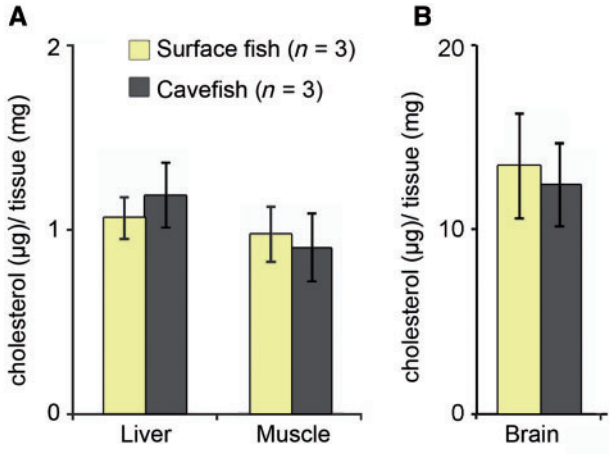

Figure 6. Total cholesterol content in the liver, muscle, and brain of surface fish and cavefish. The cholesterol content of liver and muscle (A) and brain (B) were quantified by enzymatic assay according to the manufacturer's protocol and normalized to tissue weight. Relative values are mean ± SD of at least 3 independent experiments. Cavefish did not differ significantly from surface fish in any of the 3 tissues.

Availability of Data and Material

The authors confirm that all data underlying the findings are fully available without restriction. All relevant data are within the Methods, in the Additional files section, and in the SRA under accession numbers: SRR788094 for *S. angustiporus* and SRR788095 for *S. anophthalmus*.

Conflict of Interest

The authors declare that they have no competing interests.

Authors' Contributions

F.W.M. and J.H.P. conceived this study and designed the experiments. F.W.M., Y.H.Z. and C.G.Z. collected the fish samples. F.W.M. carried out the H&E staining, real-time PCR and cholesterol test. F.W.M. and T.T. prepared the cDNA libraries for RNA-seq. F.W.M. and J.H.P. performed computer analysis of RNA-seq data. F.W.M. generated all images and F.W.M. and J.H.P. wrote the manuscript. All authors read, revised, and approved the final manuscript.

Acknowledgments

We thank R. BreMiller (University of Oregon) and J. Ganz (Michigan State University) for help with neuroanatomy.

Funding

This work was financially supported by grants from the National Natural Science Foundation of China NSFC31372191 (F.W.M.), NSFC31471961 (Y.H.Z.) and NIH grants NIH R01 OD011116 (J.H.P.) and R24 RR032670 (J.H.P.). Funding agencies had no role in the design, collection, analysis, and interpretation of data; in the writing of the manuscript; or in the decision to submit the manuscript for publication.

Supplementary Material

Supplementary material can be found at https://academic.oup.com/cz.

Glossary

acat1	acetyl-coenzyme A acetyltransferase 1 (thiolase)
aga	aspartylglucosaminidase
ap1s1	adaptor-related protein complex 1, sigma 1 subunit
ap1s2	adaptor-related protein complex 1, sigma 2 subunit
ap1s3b	adaptor-related protein complex 1, sigma 3 subunit, b
ap3m1	adaptor-related protein complex 3, mu 1 subunit
ap4s1	adaptor-related protein complex 4, sigma 1 subunit
asah1a	N-acylsphingosine amidohydrolase (acid ceramidase) 1a
crh	corticotropin releasing hormone
cyp46a1	cytochrome P450, family 46, subfamily A, polypeptide 1
cyp51	cytochrome P450, family 51 (lanosterol demethylase)
ctsk	cathepsin K
dhcr24	24-dehydrocholesterol reductase
dhcr7	7-dehydrocholesterol reductase
ebp	emopamil binding protein (sterol isomerase)
faxdc2	fatty acid hydroxylase domain containing 2
fdft1	farnesyldiphosphate farnesyltransferase 1
fdps	farnesyl-diphosphate synthase
galcb	galactosylceramidase b
gla	galactosidase, alpha
glb1l	galactosidase, beta 1-like
hmgcr	3-hydroxy-3-methylglutaryl-CoA reductase
hmgcs	3-hydroxy-3-methylglutaryl-CoA synthase
hsd17b7	hydroxysteroid (17-beta) dehydrogenase 7
idi1	isopentenyldiphosphate isomerase 1
lbr	lamin-B receptor
lss	lanosterol synthase
mc4r	melanocortin-4-receptor
msmo1	methylsterol monooxygenase 1
mvd	mevalonate-diphosphate decarboxylase
mvk	mevalonate kinase
nsdhl	NAD(P) dependent steroid dehydrogenase-like
pmvk	phosphomevalonate kinase
pomc	proopiomelanocortin
ppt1	palmitoyl-protein thioesterase 1
sc5d	sterol-c5-desaturase (lathosterol oxidase)
sgsh	N-sulfoglucosamine sulfohydrolase
sqle	squalene monooxygenase
srebf	sterol regulatory element-binding factor
sst	somatostatin
trh	thyrotropin releasing hormone
tm7sf2	transmembrane 7 superfamily member 2

References

Aspiras AC, Rohner N, Martineau B, Borowsky RL, Tabin CJ, 2015. Melanocortin 4 receptor mutations contribute to the adaptation of cavefish to nutrient-poor conditions. *Proc Natl Acad Sci USA* **112**:9668–9673.

Audic S, Claverie JM, 1997. The significance of digital gene expression profiles. *Genome Res* **7**:986–995.

Bodo E, Kany B, Gaspar E, Knuver J, Kromminga A et al., 2010. Thyroid-stimulating hormone, a novel, locally produced modulator of human epidermal functions, is regulated by thyrotropin-releasing hormone and thyroid hormones. *Endocrinology* **151**:1633–1642.

De Groef B, Geris KL, Manzano J, Bernal J, Millar RP et al., 2003. Involvement of thyrotropin–releasing hormone receptor, somatostatin receptor subtype 2 and corticotropin–releasing hormone receptor type 1 in the control of chicken thyrotropin secretion. *Mol Cell Endocrinol* **203**:33–39.

Dietschy JM, Turley SD, 2004. Thematic review series: brain Lipids. Cholesterol metabolism in the central nervous system during early development and in the mature animal. *J Lipid Res* **45**:1375–1397.

Elipot Y, Hinaux H, Callebert J, Launay JM, Blin M et al., 2014. A mutation in the enzyme monoamine oxidase explains part of the Astyanax cavefish behavioural syndrome. *Nat Commun* **5**:3647.

Faust PL, Kovacs WJ, 2014. Cholesterol biosynthesis and ER stress in peroxisome deficiency. *Biochimie* **98**:75–85.

Gross JB, 2012. The complex origin of Astyanax cavefish. *BMC Evol Biol* **12**:105.

Harris AR, Christianson D, Smith MS, Fang SL, Braverman LE et al., 1978. The physiological role of thyrotropin–releasing hormone in the regulation of thyroid-stimulating hormone and prolactin secretion in the rat. *J Clin Invest* **61**:441–448.

Hüppop K, 2005. Adaptation to low food. In: Culver DC, White WB, editors. *Encyclopedia of Caves*. Amsterdam: Elsevier Academic Press, 4–10.

Ivanisevic J, Siuzdak G, 2015. The role of metabolomics in brain metabolism research. *J Neuroimmune Pharmacol* **10**:391–395.

Jeffery WR, 2009. Regressive evolution in *Astyanax* cavefish. *Annu Rev Genet* **43**:25–47.

Krishnan J, Rohner N, 2017. Cavefish and the basis for eye loss. *Philos Trans R Soc Lond B Biol Sci* **372**. doi:10.1098/rstb.2015.0487.

Langmead B, 2010. Aligning short sequencing reads with Bowtie. *Curr Protoc Bioinformatics*. doi:10.1002/0471250953.bi1107s32.

Lund EG, Xie C, Kotti T, Turley SD, Dietschy JM et al., 2003. Knockout of the cholesterol 24-hydroxylase gene in mice reveals a brain-specific mechanism of cholesterol turnover. *J Biol Chem* **278**:22980–22988.

Martin MG, Pfrieger F, Dotti CG, 2014. Cholesterol in brain disease: sometimes determinant and frequently implicated. *EMBO Rep* **15**:1036–1052.

McGaugh SE, Gross JB, Aken B, Blin M, Borowsky R et al., 2014. The cavefish genome reveals candidate genes for eye loss. *Nat Commun* **5**:5307.

Meng F, Braasch I, Phillips JB, Lin X, Titus T et al., 2013a. Evolution of the eye transcriptome under constant darkness in Sinocyclocheilus cavefish. *Mol Biol Evol* **30**:1527–1543.

Meng F, Zhao Y, Postlethwait JH, Zhang C, 2013b. Differentially-expressed opsin genes identified in Sinocyclocheilus cavefish endemic to China. *Curr Zool* **59**:170–174.

Menuet A, Alunni A, Joly JS, Jeffery WR, Retaux S, 2007. Expanded expression of Sonic hedgehog in Astyanax cavefish: multiple consequences on forebrain development and evolution. *Development* **134**:845–855.

Mitsche MA, McDonald JG, Hobbs HH, Cohen JC, 2015. Flux analysis of cholesterol biosynthesis in vivo reveals multiple tissue and cell-type specific pathways. *Elife* **4**: e07999.

Moran D, Softley R, Warrant EJ, 2014. Eyeless Mexican cavefish save energy by eliminating the circadian rhythm in metabolism. *PLoS ONE* **9**: e107877.

Mortazavi A, Williams BA, McCue K, Schaeffer L, Wold B, 2008. Mapping and quantifying mammalian transcriptomes by RNA-Seq. *Nat Methods* **5**:621–628.

Pfrieger FW, 2003. Cholesterol homeostasis and function in neurons of the central nervous system. *Cell Mol Life Sci* **60**:1158–1171.

Porter FD, Herman GE, 2011. Malformation syndromes caused by disorders of cholesterol synthesis. *J Lipid Res* **52**:6–34.

Protas M, Tabansky I, Conrad M, Gross JB, Vidal O et al., 2008. Multi-trait evolution in a cave fish, *Astyanax mexicanus*. *Evol Dev* **10**:196–209.

Riedel G, 1997. The forebrain of the blind cave fish *Astyanax hubbsi* (Characidae). I. General anatomy of the telencephalon. *Brain Behav Evol* **49**:20–38.

Roder B, Teder-Salejarvi W, Sterr A, Rosler F, Hillyard SA et al., 1999. Improved auditory spatial tuning in blind humans. *Nature* **400**:162–166.

Rohner N, Jarosz DF, Kowalko JE, Yoshizawa M, Jeffery WR et al., 2013. Cryptic variation in morphological evolution: HSP90 as a capacitor for loss of eyes in cavefish. *Science* **342**:1372–1375.

Romero A, Zhao YH, Chen XY, 2009. The Hypogean fishes of China. *Environ Biol Fish* **86**:211–278.

Rosen GD, Harry JD, 1990. Brain volume estimation from serial section measurements: a comparison of methodologies. *J Neurosci Methods* **35**:115–124.

Russell DW, Halford RW, Ramirez DM, Shah R, Kotti T, 2009. Cholesterol 24-hydroxylase: an enzyme of cholesterol turnover in the brain. *Annu Rev Biochem* **78**:1017–1040.

Salin K, Voituron Y, Mourin J, Hervant F, 2010. Cave colonization without fasting capacities: an example with the fish *Astyanax fasciatus mexicanus*. *Comp Biochem Physiol A Mol Integr Physiol* **156**:451–457.

Simon V, Elleboode R, Mahe K, Legendre L, Ornelas-Garcia P et al., 2017. Comparing growth in surface and cave morphs of the species Astyanax mexicanus: insights from scales. *Evodevo* **8**:23.

Soares D, Yamamoto Y, Strickler AG, Jeffery WR, 2004. The lens has a specific influence on optic nerve and tectum development in the blind cavefish Astyanax. *Dev Neurosci-Basel* **26**:308–317.

Stahl BA, Gross JB, 2017. A comparative transcriptomic analysis of development in two Astyanax cavefish populations. *J Exp Zool B Mol Dev Evol* **328**:515–532.

Strecker U, Hausdorf B, Wilkens H, 2012. Parallel speciation in Astyanax cave fish (Teleostei) in Northern Mexico. *Mol Phylogenet Evol* **62**:62–70.

Suzuki R, Ferris HA, Chee MJ, Maratos-Flier E, Kahn CR, 2013. Reduction of the cholesterol sensor SCAP in the brains of mice causes impaired synaptic transmission and altered cognitive function. *PLoS Biol* **11**: e1001532.

Tao YX, 2010. The melanocortin-4 receptor: physiology, pharmacology, and pathophysiology. *Endocr Rev* **31**:506–543.

Wang J, Duncan D, Shi Z, Zhang B, 2013. WEB-based GEne SeT AnaLysis Toolkit (WebGestalt): update 2013. *Nucleic Acids Res* **41**:W77–W83.

Weber LW, Boll M, Stampfl A, 2004. Maintaining cholesterol homeostasis: sterol regulatory element-binding proteins. *World J Gastroenterol* **10**: 3081–3087.

Windsor SP, Tan D, Montgomery JC, 2008. Swimming kinematics and hydrodynamic imaging in the blind Mexican cave fish *Astyanax fasciatus*. *J Exp Biol* **211**:2950–2959.

Xiao H, Chen SY, Liu ZM, Zhang RD, Li WX et al., 2005. Molecular phylogeny of Sinocyclocheilus (Cypriniformes: Cyprinidae) inferred from mitochondrial DNA sequences. *Mol Phylogenet Evol* **36**:67–77.

Xie C, Mao X, Huang J, Ding Y, Wu J et al., 2011. KOBAS 2.0: a web server for annotation and identification of enriched pathways and diseases. *Nucleic Acids Res* **39**:W316–W322.

Yang JX, Chen XL, Bai J, Fang DM, Qiu Y et al., 2016. The Sinocyclocheilus cavefish genome provides insights into cave adaptation. *BMC Biol* **14**:1.

Yoshizawa M, Goricki S, Soares D, Jeffery WR, 2010. Evolution of a behavioral shift mediated by superficial neuromasts helps cavefish find food in darkness. *Curr Biol* **20**:1631–1636.

Yoshizawa M, Robinson BG, Duboue ER, Masek P, Jaggard JB et al., 2015. Distinct genetic architecture underlies the emergence of sleep loss and prey-seeking behavior in the Mexican cavefish. *BMC Biol* **13**:15.

Zhao Y, Zhang C, 2009. *Endemic Fishes of Sinocyclocheilus (Cypriniformes: Cyprinidae) in China: Species Diversity, Cave Adaptation, Systematics and Zoogeography*. Beijing: Science Press.

Zhao YH, Gozlan RE, Zhang CG, 2011. Out of sight out of mind: current knowledge of Chinese cave fishes. *J Fish Biol* **79**:1545–1562.